THE GEM-MARS GCM: CURRENT STATUS AND EVALUATION.

L. Neary and F. Daerden, *Belgian Institute for Space Aeronomy, (lori.neary@aeronomie.be)*.

Introduction

GEM-Mars is a global general circulation model for the Mars atmosphere, based on the dynamical core of the Global Environmental Multiscale model, part of the operational Canadian weather forecast system. It is a grid-point model using a semi-Lagrangian advection scheme with semi-implicit time integration. This allows for a relatively long timestep while maintaining stability. The option to run with hydrostatic or non-hydrostatic formulation of the primative equations gives the capability of running at multiple horizontal scales down to the mesoscale. The advantage of using code from an operational weather prediction model is that it is fully parallelized and efficient. The results presented here are using the most recent version of the dynamical core v4.2.0, using a horizontal resolution of $4°\times4°$, 103 vertical levels up to $\sim$150 km and a 30 minute timestep. The model also includes a multi-layered soil model for heat conduction, including a subsurface ice table in the (sub)polar regions, parameterizations for the surface layer (Monin-Obhukov similarity theory), planetary boundary layer (PBL) turbulent diffusion, gravity wave drag parameterization, eddy and molecular diffusion. A basic gas-phase atmospheric chemistry package is also included.

A brief description of the basic physical parameterisations will be given and some comparisons to the Thermal Emission Spectrometer (Smith, 2002), Mars Climate Sounder (McCleese et al., 2007), Gamma Ray Spectrometer (Kelly et al., 2006) and the Viking landers.

Radiation

The radiative transfer code in GEM-Mars includes CO_2 absorption and emission in the 15 μm band as given in Hourdin (1992) and applies a two-stream method in visible and IR wavelengths through dust, applying the dust optical properties from Wolff et al. (2006, 2009). For these simulations, the dust is prescibed using the MGS dust scenario (Forget et al., 1999) with a Conrath shape profile (see Figure 1). In parallel, a version of the model with active dust lifting has been developed (see Daerden et al., this workshop). Because of the vertical extent of the model, non-LTE corrections are made using the work of Lopez-Valverde et al. (1994) and UV/EUV heating are also included in the upper atmosphere.

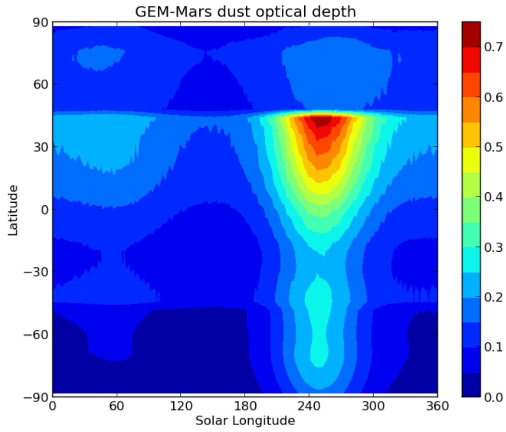

Figure 1: GEM-Mars zonal mean dust optical depth based on the MGS scenario.

General circulation

Figure 2 shows the basic state of the atmosphere for 4 seasons, zonal mean temperatures and winds. The signature westerly jets at the equinoxes are seen as in other GCM models for Mars as well as the winter polar warmings at the solstices.

Comparison with MCS temperatures and dust

GEM-Mars temperature and dust profiles have been extracted at the same times and locations of 3 years of MCS profiles and averaged into latitude and L_s bins. Figure 3 shows the comparison for the 4 seasons at 3 latitude bands, north polar, equatorial and south polar regions. Considering the use of climatological dust, the temperature agreement is reasonable. Improved results in the latter part of the year are expected with the implementation of active dust lifting. The temperatures in the equatorial region are in the best agreement, while the north polar region is the most sensitive to dust profiles used. Figure 4 gives the comparison of MCS dust extinction for reference.

Water Cycle

The GEM-Mars model includes a northern polar permanent water ice cap and a simple evaporation/condensation

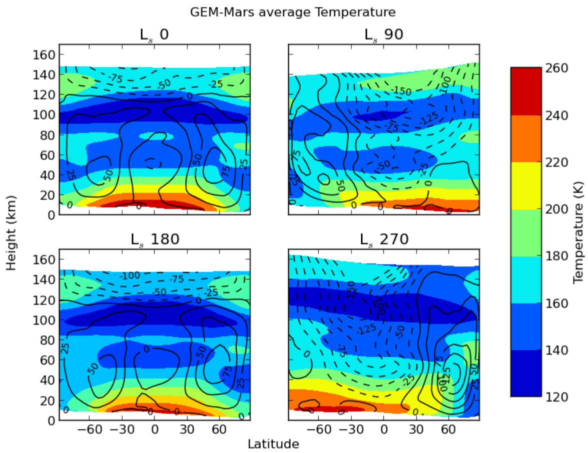

Figure 2: GEM-Mars zonal mean temperature (coloured contours) and zonal winds (black contours, solid lines are westerly winds) for L_s 0, 90, 180 and 270.

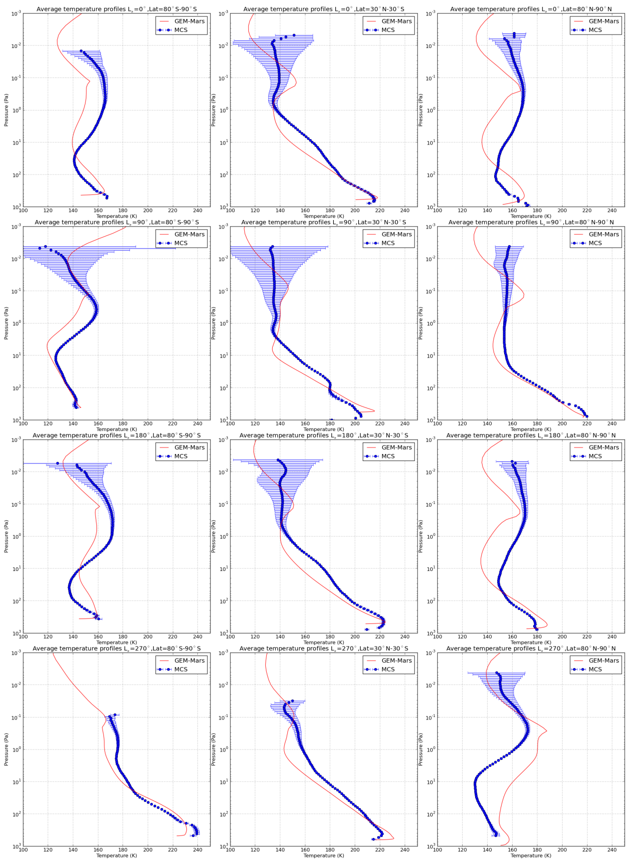

Figure 3: comparison of GEM-Mars and MCS average profiles of temperature for 4 seasons 3 latitude bands: from top to bottom L_s 0, 90, 180 and 270. Left column is 70-90N, centre column 10N-10S, right column 70-90S.

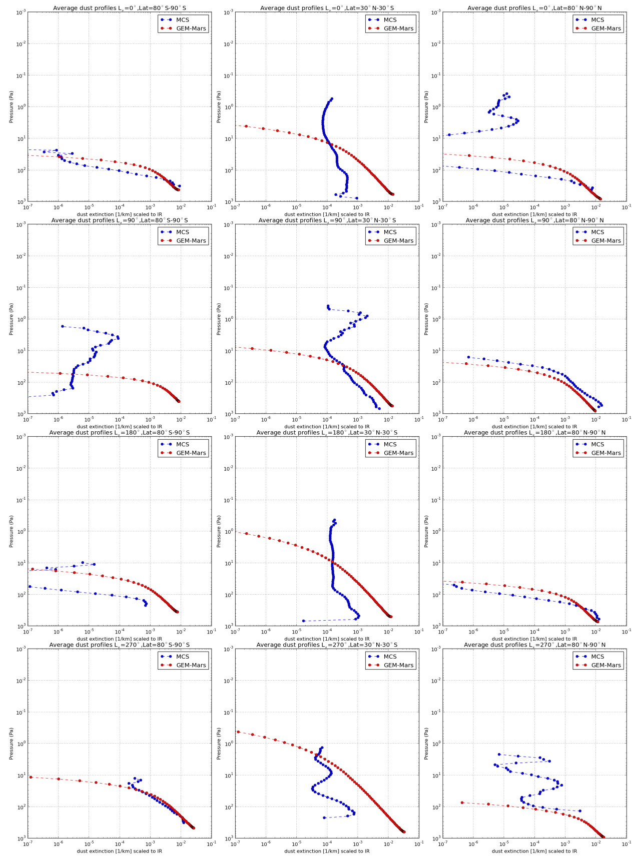

Figure 4: comparison of GEM-Mars and MCS average profiles of dust extinction for 4 seasons 3 latitude bands: from top to bottom L_s 0, 90, 180 and 270. Left column is 70-90N, centre column 10N-10S, right column 70-90S.

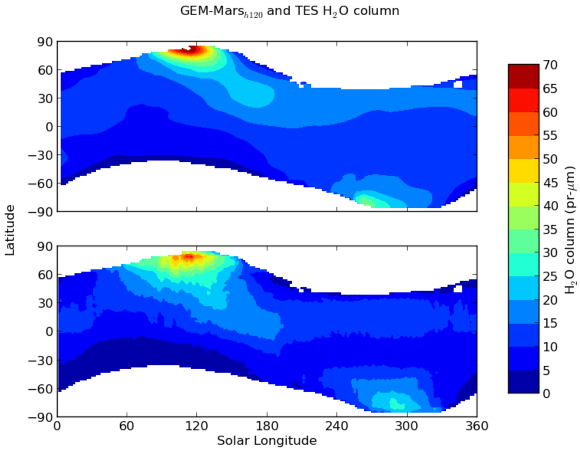

Figure 5: Zonal mean water column, GEM-Mars (top) and TES (bottom).

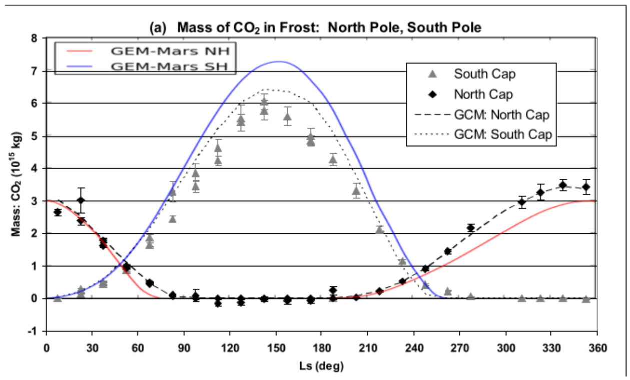

Figure 6: CO_2 ice on caps compared with GRS data from Kelly et al., 2006.

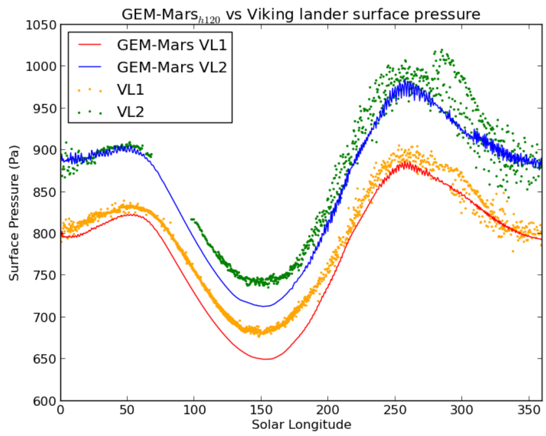

Figure 7: Surface pressure compared with Viking landers I and II.

scheme as well as bulk water ice cloud formation. The total column amount of water vapour is compared with TES in Figure 5, showing the basic structure is represented. The water cycle is sensitive to the prescribed water ice albedo used as well as parameters used in the sub-surface model.

CO_2 Cycle

In the polar regions in winter, as much as 30% of the CO_2 in the atmosphere condenses onto the caps and then sublimates again in the spring. Figure 6 has the model CO_2 surface ice amount overlaid on the figure from Kelly et al. (2006) which shows data derived from GRS measurements. There is a slight over-prediction of condensation on the southern cap but overall the agreement is acceptable. The behaviour of the CO_2 cycle is dependent on the parameters used in the sub-surface model and can be adjusted to better match the data.

As so much of the CO_2 in the atmosphere condenses and sublimates, a change in surface pressure can be seen. The surface pressure change is derived from the mass exchange between atmosphere and polar caps. Figure 7 compares daily average surface pressure with that measured at the two Viking lander sites. The basic pattern agrees although the decrease in pressure at L_s 150 is slightly too deep.

Discussion and conclusions

Overall, the GEM-Mars model is able to reproduce the basic state of the atmosphere including general circulation, temperature and seasonal cycles of pressure,

CO_2 and H_2O. The implementation of active dust lifting should improve temperatures, especially in the dust storm season.

References

[1] Forget, F., F. Hourdin, R. Fournier, C. Hourdin, O. Talagrand, M. Collins, S. R. Lewis, P. L. Read, and J.P. Huot (1999), Improved general circulation models of the Martian atmosphere from the surface to above 80 km, J. Geophys. Res., 104, 24,15524,175, doi:10.1029/1999JE001025

[2] Hourdin, F. (1992). A new representation of the absorption by the CO2 15-m band for a Martian general circulation model. Journal of Geophysical Research: Planets 97, 1831918335.

[3] Kelly, N. J., W. V. Boynton, K. Kerry, D. Hamara, D. Janes, R. C. Reedy, K. J. Kim, and R. M. Haberle (2006), Seasonal polar carbon dioxide frost on Mars: CO2 mass and columnar thickness distribution, J. Geophys. Res., 111, E03S07, doi:10.1029/2006JE002678.

[4] Lpez-Valverde M. and M. Lpez-Puertas (1994), A non local thermodynamic equilibrium radiative transfer model for infrared emissions in the atmosphere of Mars 1. Theoretical basis and nighttime populations of vibrational levels, J. Geophys. Res., 99, 13,093-13,115.

[5] McCleese, D. J., J. T. Schofield, F. W. Taylor, S. B. Calcutt, M. C. Foote, D. M. Kass, C. B. Leovy, D. A. Paige, P. L. Read, and R. W. Zurek (2007), Mars Climate Sounder: An investigation of thermal and water vapor structure, dust and condensate distributions in the atmosphere, and energy balance of the polar regions, J. Geophys. Res., 112, E05S06, doi:10.1029/2006JE002790

[6] Smith, M.D. (2002). The annual cycle of water vapor on Mars as observed by the Thermal Emission Spectrometer. Journal of Geophysical Research 107.

[7] Wolff, M. J., et al. (2006), Constraints on dust aerosols from the Mars Exploration Rovers using MGS overflights and MiniTES, J. Geophys.Res., 111, E12S17, doi:10.1029/2006JE002786.

[8] Wolff, M. J., M. D. Smith, R. T. Clancy, R. Arvidson, M. Kahre, F. Seelos, S. Murchie, and H. Savijrvi (2009), Wavelength dependence of dust aerosol single scattering albedo as observed by the Compact Reconnaissance Imaging Spectrometer, J. Geophys. Res., 114,E00D04, doi:10.1029/2009JE003350.